



Multivariable control of regeneratively-cooled scramjet engine with two-stage kerosene injection based on H_∞ method

Chengkun Lv^a, Juntao Chang^{a,*}, Daren Yu^a, Hao Liu^b, Cheng Xu^{c,**}

^a Harbin Institute of Technology, 150001, Heilongjiang, PR China

^b Xi'an Aerospace Propulsion Institute, 710100, Xi'an, PR China

^c Beijing Research Institute of Mechanical and Electrical Engineering, 100074, Beijing, PR China

ARTICLE INFO

Keywords:

Regeneratively-cooled scramjet engine
Multivariable control
 H_∞ method
Switching controller

ABSTRACT

Aimed at diversity of hypersonic flight mission, this paper discusses the multivariable control of regeneratively-cooled scramjet engine with two-stage kerosene injection for both safety operation and high performance. Firstly, the multivariable control strategy is proposed to solve the inlet unstart and overtemperature control issues. There are two linear models identified for different control objects because of the control strategy. Among them, the inputs are two-stage fuel equivalence ratios, and the outputs are thrust, inlet steady margin, and thrust and kerosene temperature at cooling channels outlet, respectively. Secondly, H_∞ multivariable control method is introduced. The standard H_∞ control problem with structural uncertainty is constructed in detail. In order to settle the issue that the control strategy selects various controlled output variables under different flight missions, a switching controller based on controller output reset is proposed. Lastly, not only thrust and steady margin control loop, but also thrust and fuel temperature control loop of the regeneratively-cooled scramjet engine are established. Simultaneously, the switching system with the two control loops is designed in this paper. Simulation results indicate that rapid responses of control system, smooth and steady switching between different loops are realized. The engine with control system can operate steadily with high performance at both specific and variable operating conditions.

1. Introduction

With the merits of both high specific impulses and high speed in the atmosphere, scramjets are regarded as one of the most ideal air-breathing propulsion devices in hypersonic flight [1]. Especially for the vehicle need to launch and land horizontally, the mature scramjet technology makes it possible to the combined cycle propulsion system [2]. Engine performance is affected by many factors, among which improving the engine cycle mode is an important means to enhance engine performance [3,4]. In order to solve the overtemperature of the combustion for scramjet flying at high Mach, generally over Mach 5, the regeneratively-cooled scramjet engine that cooled by the on-board hydrocarbon fuel is investigated in detail [5,6]. The special problems of regeneratively-cooled scramjet engine bog down the complicated design of the control system for scramjet. On the one hand, under broad flight operating conditions, complex issues such as the shock wave movement in the inlet [7] and combustion modes in the combustor [8] are

frequently discussed in researches of scramjet control. On the other hand, the coupling characteristics of cooling process and the structure of two-stage kerosene injection lead to a large dynamic inertial of the regeneratively-cooled scramjet engine, which makes the control system design unique [9]. In view of the above, the control system of the regeneratively-cooled scramjet engine is a multivariable one with multiple control objects under a wide range of operating conditions.

Designers of control systems pay close attention to the analysis of characteristics and the control-oriented model of the controlled plant. In order to make scramjets adapt to the serious aerothermodynamic environment in a various flight operating conditions, researchers have carried out a large number of experiments, numerical simulations and modeling studies on inlets, combustions and other components. Dalle [10] presented a reduced-order model that predicts the solution of a steady two-dimensional supersonic flow. Xing [11] demonstrated that the boundary layer bleeding could prevent the shock train from moving upstream. Xu [12] observed a rapid movement of the shock train when its forward climbing and investigated the mechanism and limits for it.

* Corresponding author.

** Corresponding author.

E-mail address: changjuntao@hit.edu.cn (J. Chang).

Nomenclature			
e	error signal	w	external input signal
F	thrust	W_1	performance weight function
F_r	command signal of F	W_2	input weight function
G	transfer function	W_3	output weight function
G_p	transfer function with uncertainty	W_f	uncertainty weight function
K	controller	x	raw data
Ma	Mach number	x_0	value at initial point
P	generalized controlled plant	y_r	command signal
S	sensitivity function	y_Δ	uncertainty input signal
SF	scale transformation	z	performance output signal
SF-1	inverse scale transformation	δ	switch command signal
T	complementary sensitivity function	φ_1	first stage fuel equivalence ratio
T_{out}	kerosene temperature at cooling channels outlet	φ_2	second stage fuel equivalence ratio
$T_{out,r}$	command signal of T_{out}	γ	H ∞ index
u	controller output signal	$\bar{\sigma}$	maximum singular value
u_Δ	uncertainty output signal	ξ	inlet steady margin
v	controller input signal	ξ_r	command signal of ξ
		Δ_I	structured multiplicative input uncertainty

Huang [13] investigated a three-dimensional scramjet isolator and the numerical results indicated that unstart phenomenon would take place after the back pressure was sufficiently large. Li [14] studied the oscillation characteristics of the shock train in an isolator. Wang [15] investigated combustion instabilities of the scramjet combustor mounted on a Mach 2.1 direct-connect test. Tian [16] studied the effect of equivalence ratio and fuel distribution on combustion performance of the dual-mode scramjet engine by numerical simulations and experiments. Combustor modes greatly affected the inlet boundary conditions, and combustion mode transition can be explained as balance feedback between combustion and flow [17–19]. The studies on the characteristics of inlet and combustor of scramjet are helpful for the design of control system. In addition, the modeling of scramjet is vital too. Torrez [20] developed an improved method to compute the thrust of a dual-mode scramjet that combustor operated both in subsonic and supersonic. For scramjet with regeneratively-cooled combustor, the experimental of the system dynamics analysis demonstrated that the management of engine cooling by the fuel is a challenge, because it is absolutely counter-intuitive in classical heat exchangers to observe that coolant temperature increases with coolant flow rate [5]. In order to work out the potential control issue of the engine, Ma [6,21], set up a one-dimensional model of regeneratively-cooled scramjet with two-stage kerosene injection, which could solve the problem of overtemperature by rationally distributing two kerosene inputs. In general, the characteristic analysis and control-oriented modeling of the regeneratively-cooled scramjet engine are beneficial to the control system design.

Researches on control of scramjets can be briefly divided into three parts, which are inlet control, combustor control and engine control. For decades, inlet unstart has troubled the flight test of CIAM/NASA Mach 6.5 scramjet, X-51 A and so on, which could lead to a large drop of thrust or even engine flameout. Varshney [22] studied unstart control in scramjet, and the results shown that unstart was avoided by releasing high pressure fluid from the slots which were designed on the wall of isolator. Liu [23] adopted the method of energy addition to improve the restarting capability of hypersonic inlet. Besides, it is a feasible method by controlling the location of shock train which is closely linked with unstart. In literature [24], the shock train in a direct-connect scramjet was controlled by a proportional-derivative (PD) controller, when the shock train location was obtained by either a direct measurement or a predictive one. Besides, Li [25] investigated the pressure ratio method, static pressure summation method and backpressure method for locating the shock train, so that a closed-loop PI controller is designed in a direct-connect wind tunnel. Different from the inlet, the research on

combustor control mainly focused on the combustion performance of scramjet. In fact, the closed-loop control of combustor is mostly related to the overall performance output such as thrust of the engine and temperature of the combustor. Therefore, all information is presented at the part of scramjet engine control. Qi [26] conducted thrust control and safety protection control of inlet buzz. Once inlet buzz appears, safety protection control loop can generate a suitable correction signal to replace the original thrust command which makes engine operate dangerously. Cao [27,28] presented switching control method based on strategies of Min value and integral initial values resetting. It can ensure a smooth switch between thrust and unstart loop. Echols [29] introduced multivariable control in the design of control system. An [30] proposed a low-dimension full-envelope adaptive control. Goel [31] pursued retrospective cost adaptive control to make engine operate safely when it was closed to unstart boundary of the scramjet combustor. Considering that the single controller cannot satisfy the control effect of the engine in a large range, the switched control method has been studied extensively [32,33]. Among them, the multiple Lyapunov function approach based on average dwell time is proposed to study switched linear parameter-varying (LPV) systems and a good switched control effects have been achieved in aero engine and hypersonic aircraft models [34, 35]. In addition, Ma [9] designed the multi-objective coordinated control of regeneratively-cooled scramjet with two-stage kerosene injection, which could keep engine operating safe under high performance by the switch rules and algorithm between thrust regulation, steady margin protection, restart recovery, temperature protection and over-temperature recovery sub-control loop. However, the coupling effects of two-stage kerosene injection could not be reflected in the single variable controller, and the algorithm of engine optimization relies on complex switching rule. Meanwhile, the verification of the controller was only completed under the specific operating conditions. So far, the research for the field of scramjet engine control can be summed up as follows: (1) The control system was mostly investigated based on no-cooled scramjet engine, and there is little discussion on regeneratively-cooled one. (2) Control objectives of closed-loop system were mainly focused on thrust and unstart but with less related researches about temperature problem. (3) Researches on regeneratively-cooled scramjet engine control still relied on the multi-loop single variable controller switching method. The coupling effects of the two-stage kerosene injection in thrust tracking, unstart, and overtemperature issues were hardly considered, and the validation in variable operating conditions was not completed.

Compared with existing studies, the main contributions of this work are as follows. Firstly, this paper adopts multivariable control method to

solve the control problem of the regeneratively-cooled scramjet engine with two-stage kerosene injection. This control issue is caused by a new type of engine. The innovation of our research is to apply existing control methods to new objects and solve special control problems. The control problem of the engine is designed as two multivariable control loops at different Mach numbers, that is, the thrust and steady margin control loop works at low Mach numbers, as well as the thrust and fuel temperature control loop operates at high Mach numbers. By adjusting two stage kerosene allocation proportion reasonably, the safety and performance problems can be solved simultaneously. Secondly, a multivariable switching controller based on controller output signal reset is discussed in this paper, which can deal with the contradiction between high performance and safe operation of the engine under different operating conditions. In addition, the whole system is verified under variable operating conditions from Mach 4 to Mach 7. The results show that the control system can track the command signal well and ensure the stability of the switching process.

This paper is organized as follow. The control problem is stated in Section 2. In Section 3, the model of engine is introduced in detail, and linear models are obtained based on control strategy. Section 4 shows the knowledge of the control methodology. The design and validation of control system is stated in Section 5. Section 6 presents the conclusion.

2. Problem statement

The purpose of this paper is to solve the problem of guaranteeing thrust performance and safety performance of the special regeneratively-cooled scramjet engine with two-stage kerosene injection during flight. The control problem is caused by a new type of engine. This kind of engine involves the complex multi-process of cooling and combustion coupling, in which kerosene is injected into the combustion after cooling the wall of engine. Different from the ordinary one, the regeneratively-cooled scramjet engine increases the overall energy utilization and improves the internal thermal environment of the engine through the cooling channel. However, these engines have always faced with a positive feedback problem, namely that the higher temperature of combustion, the more cooling kerosene is needed, then the more heat will be released into the combustion resulting in a higher temperature. Thus, regeneratively-cooled technology also leads to significant control problems. Besides, the cracking of kerosene in the cooling channel brings great changes to the dynamic characteristics of the engine under high temperature conditions. But, the special cooling channel structure of the two-stage kerosene injections provides a completely new degree of freedom for the engine and affects the design of the control system. In a word, the regeneratively-cooled scramjet engine is facing a new control problem that affects the safety of operation. This problem is different from the general overtemperature of the combustion, but it is a fresh one triggered when the regeneratively-cooled technology is used to avoid the overtemperature. Of course, traditional inlet safety problems also plague

the regeneratively-cooled scramjet engine controller. Aiming at the above problems, we have established the 1-D model of regeneratively-cooled scramjet engine with two-stage kerosene. This paper focuses on applying control methods to solve the contradiction of thrust and safety for the special regeneratively-cooled scramjet engine.

3. Problem formulation

3.1. Engine model

In this paper, the one-dimensional (1-D) model of the regeneratively-cooled scramjet engine for investigation is described in Ref. [6]. Fig. 1 demonstrates the schematic of regeneratively-cooled scramjet engine, where the dashed line represents the flow path of kerosene.

The 1-D unsteady model can deal with problems such as variable area, fuel addition, combustion heat release, variable specific heat, inflow air vitiation component, wall friction and mixing efficiency. The main content of the model including isolator shock train model, oblique shock wave modification and combustion heat release distribution. In addition, the model can calculate detailed scramjet combustor 1-D flow field characteristic under the certain scramjet combustor configuration and multiple inflow conditions. The safety boundary codetermined by unstart and over-temperature is conducted using this model. Interested readers can learn more about the modeling details of the scramjet with active cooling in Ref. [6,21]. Here, the model can be expressed in the following form

$$\begin{cases} F = f_1(Ma, \varphi_1, \varphi_2) \\ \xi = f_2(Ma, \varphi_1, \varphi_2) \\ T_{out} = f_3(Ma, \varphi_1, \varphi_2) \end{cases} \quad (1)$$

where F is thrust, ξ is inlet steady margin, T_{out} is kerosene temperature at cooling channels outlet, Ma is Mach number, φ_1 is first stage fuel equivalence ratio, and φ_2 is second stage fuel equivalence ratio.

The flight conditions of the 1-D model are obtained by CFD calculation according to the data given in Refs. [36,37]. The flight conditions of vehicle and isolator equivalence entrance conditions are shown in Table 1, where Ma is Mach number, P is dynamic pressure, P_t is total pressure, and T_t is total temperature.

One-dimensional (1-D) model for regeneratively-cooled scramjet en-

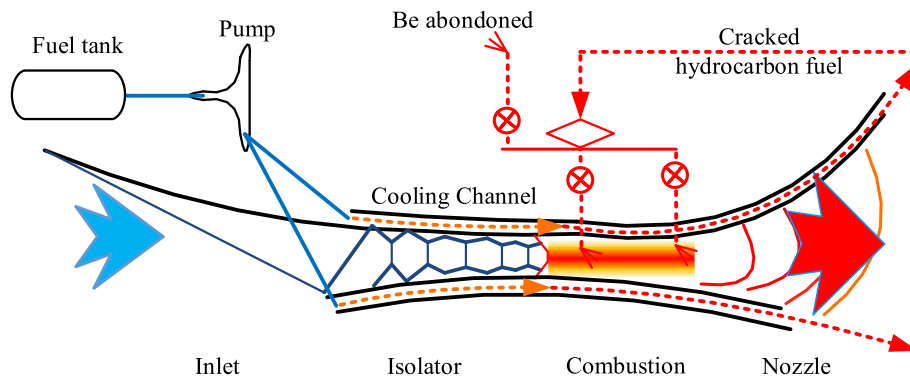


Fig. 1. Schematic of regeneratively-cooled scramjet engine [6].

engine is a multi-process coupled model. It can simulate flow and combustion process in engine, the coupled heat transfer relationship between cooling and combustion, heat conduction through the engine walls and kerosene flowing in cooling channels. According to previous research [6], thrust increments generated by φ_1 is higher than ones generated by φ_2 . But allowable φ_1 is limited, especially during low Mach number. When engine operates close to unstart boundary, φ_1 cannot increase continually. Maximum energy that can be added in engine is enhanced by increasing φ_2 so that maximum thrust can be improved. For ξ , it is the safety target of the engine control, because unstart mode is disastrous for the engine. As discussed in Refs. [9], ratio of pressure located in combustor to pressure at isolator inlet is treated as monitor data in the 1-D model. When pressure ratio reaches maximum, isolator cannot stand the backpressure of combustor, and unstart will occur. At the moment, margin ξ equals 0. The larger ξ is, the farther distance away from unstart boundary is, the safer operating state is, but the optimal performance of the engine does not vary in this way. The maximum of ξ is 1. In addition, Ref [9] gives the calculation results of the model under specific working conditions. When Mach number is equal to 5, Fig. 2 shows the isothermal of T_{out} for 1-D regeneratively-cooled engine model under different φ_1 and φ_2 . It reveals that T_{out} exists an obvious drop with φ_2 increasing, but this phenomenon cannot be seen by increasing φ_1 .

3.2. Control strategy and linearization

The particularity of the control problem for the regeneratively-cooled scramjet engine comes from both the wide flight conditions and the complex cooling channel structure. First of all, for the scramjet engine with two-stage injection, the kerosene injected into the combustion is limited by the unstart boundary of the inlet at low Mach number. The engine with high performance has a normal shock wave close to the critical boundary. The goal of the control system is to ensure thrust performance and inlet starting. Secondly, when engines operate at high Mach number, the control problem of the engine is to ensure the thrust performance under the maximum cooling kerosene temperature limit. At this time, there is no normal shock wave in the inlet, which means unstart of inlet will not happen. The main consideration of safety is transferred from inlet to combustor. Thus, the issue of engine safe operation is overtemperature. In brief, the engine with two-stage kerosene injection has different control problems in flight conditions, so it is necessary to choose control strategies as follow:

- 1). At low Mach number, the multivariable control system controls the engine thrust F and inlet steady margin ξ through the first stage fuel equivalence ratio φ_1 and second stage fuel equivalence ratio φ_2 .
- 2). At high Mach number the multivariable control system controls the engine thrust F and kerosene temperature at cooling channels outlet T_{out} through the first stage fuel equivalence ratio φ_1 and second stage fuel equivalence ratio φ_2 .

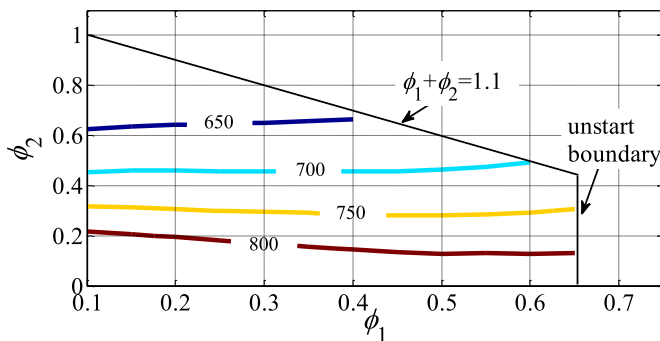


Fig. 2. Kerosene isotherm at cooling channels outlet under different φ_1 and φ_2 during $Ma_0 = 5$ for regeneratively-cooled engine [9].

In this paper, the 1-D coupling model of the regeneratively-cooled scramjet engine can fully reflect the strong nonlinear characteristics. However, it is difficult to design control system via this model. If a linear control method is applied to the regeneratively-cooled scramjet engine, a linear model must be identified. Based on observed data from the systems, system identification can transform dynamical systems to mathematical models which are called transfer function. In the controller design section, engine needs to be simplified into transfer function initially.

According to the control strategy discussed, there are two linear models that need to be identified, respectively at low Mach number and high Mach number. For fixed geometry engine with two-stage kerosene injection, controlled variable is only fuel equivalence ratio at each stage injector. Hence, inputs of transfer functions include the first stage fuel equivalence ratio φ_1 and second stage fuel equivalence ratio φ_2 . Its outputs include thrust F , inlet steady margin ξ , and kerosene temperature at cooling channels outlet T_{out} . The controlled outputs are F and ξ at low Mach number, but F and T_{out} at high Mach number. Further, the specific working conditions and input variables of the linear model identification are shown in Table 2.

In order to facilitate the design of the control system, the linear model needs to be normalized. It is worth noting that the outputs of the regeneratively-cooled scramjet engine are affected by the inputs in different direction. For less difficulty of identification for the linear model. The fixed point during 0–20 s in Table 2 is defined as the initial point (i.e., zero point in normalized data). Therefore, all the input and output parameters are scaled as follow

$$\bar{x} = (x - x_0) / \max(\text{abs}(x - x_0)) \quad (2)$$

where x is the raw data, x_0 is the value at initial point and $\max(\text{abs}(x - x_0))$ is the maximum absolute value of x relative to the starting point x_0 .

On the basis of 1-D model for regeneratively-cooled scramjet engine, unsteady simulations are conducted at different cases in Table 2 and identification data is obtained. The comparisons of normalized dynamic responses between 1-D and linear model are shown in Fig. 3-Fig. 4. In fact, the safety problem always happens near special operating conditions, thus, the φ_1 and φ_2 we considered cannot change a lot.

At Mach 4.5, the accuracy of the thrust F and steady margin ξ is acceptable and can meet the requirements of controller design. At Mach 6, due to the complicated cracking process of the kerosene, the engine has strong nonlinearity at 60 and 80 s. Fig. 4 indicates that the linear model cannot match the 1-D model in this condition. However, the variation trend of the linear model is consistent with the engine. In this paper, robust control is adopted to design the control system, which has a good control effect on the uncertainty and unmodeled part of the regeneratively-cooled scramjet engine. Therefore, the identified linear model can fully satisfy the requirements of control system design.

At low Mach number, the linear model of the engine can be expressed as:

$$\begin{bmatrix} F \\ \xi \end{bmatrix} = \begin{bmatrix} f_{11}(s) & f_{12}(s) \\ f_{21}(s) & f_{22}(s) \end{bmatrix} \begin{bmatrix} \varphi_1 \\ \varphi_2 \end{bmatrix} \quad (3)$$

Table 2

The specific working conditions and input variables of the linear model identification.

Time (s)	Case 1 (Ma 4.5)		Case 2 (Ma 6)		Case 3 (Ma 4.5)		Case 4 (Ma 6)	
	φ_1	φ_2	φ_1	φ_2	φ_1	φ_2	φ_1	φ_2
0–20	0.4338	0.10	0.3538	0.50	0.30	0.1	0.15	0.45
20–40	0.4438	0.12	0.3638	0.51	0.31	0.11	0.16	0.46
40–60	0.4338	0.12	0.3538	0.49	0.29	0.11	0.17	0.46
60–80	0.4270	0.11	0.3595	0.50	0.31	0.09	0.15	0.44
80–100	0.4394	0.10	0.3538	0.49	0.31	0.10	0.14	0.46

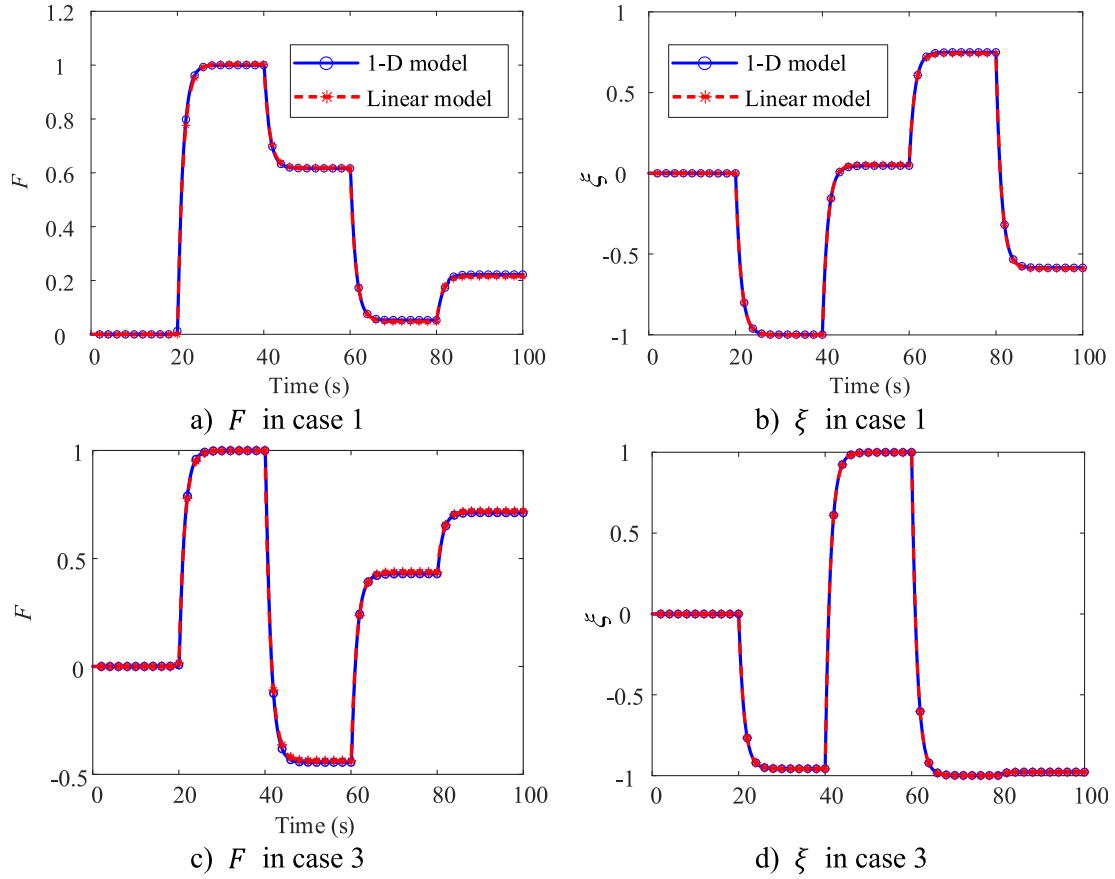


Fig. 3. The comparisons of thrust F and steady margin ξ between 1-D and linear model at Ma 4.5.

where $f_{11}(s)$ is the transfer function from φ_1 to F , $f_{12}(s)$ is the transfer function from φ_2 to F , $f_{21}(s)$ is the transfer function from φ_1 to ξ , and $f_{22}(s)$ is the transfer function from φ_2 to ξ .

At high Mach number, the linear model of the engine can be expressed as:

$$\begin{bmatrix} F \\ T_{out} \end{bmatrix} = \begin{bmatrix} g_{11}(s) & g_{12}(s) \\ g_{21}(s) & g_{22}(s) \end{bmatrix} \begin{bmatrix} \varphi_1 \\ \varphi_2 \end{bmatrix} \quad (4)$$

where $g_{11}(s)$ is the transfer function from φ_1 to F , $g_{12}(s)$ is the transfer function from φ_2 to F , $g_{21}(s)$ is the transfer function from φ_1 to T_{out} , and $g_{22}(s)$ is the transfer function from φ_2 to T_{out} .

The transfer functions obtained by identification are shown in Table 3. The first order system is used to represent the dynamic relationship between the input and output of the engine. In the expression, the molecules represent the gain, and the larger one means that the same input will result in a larger output. The parameters in the denominator represent the dynamics of the system, and the higher one shows that the system dynamic is faster.

It can be seen from the results of $f(s)$ that the linear models corresponding to Case 1 and Case 3 have very similar dynamic characteristics. The total gain of the system has not changed significantly, that is, the sum of $f_{11}(s)$ and $f_{12}(s)$ is close to the sum of $f_{21}(s)$ and $f_{22}(s)$. However, the results given by $g(s)$ show that the system dynamics of Case 4 have changed, especially in $g_{21}(s)$. This is possible to happen at high Mach number. Because the kerosene temperature at cooling channels outlet changes significantly with fuel equivalent ratio in this condition, which leads to changes in the engine dynamics. Among the four cases for identifying the linear model, the cases 1 and case 2 are close to the safety boundary of engine. Therefore, these two cases are more suitable for the control problem mainly discussed in this paper.

4. Control methodology

In this paper, the regeneratively-cooled scramjet engine is a complex multivariable system. According to the analysis of the control strategy in section 2.1, the control variables are $[\varphi_1 \ \varphi_2]^T$, and the output variables are $[F \ \xi]^T$ or $[F \ T_{out}]^T$. Robust control is widely used in the control of multivariable systems. Among them, H_∞ technology is a theory about control system synthesis. H_∞ method transforms the control plant into a standard form at first, and then uses H_∞ norm to characterize the influence of system uncertainty and unknown disturbance on the measured output parameters with weight functions. So that, the corresponding performance index of control system design can be obtained. Meanwhile, it is significant to consider a switching method for regeneratively-cooled scramjet engine under wide flight conditions. The basic design theories of the controller are given below.

4.1. Standard H_∞ control problem

In general, H_∞ synthesis can reconstruct the whole problem into a uniform standard form, so it is also called a standard problem. The most important part of the standard problem is to obtain the generalized controlled plant, which contains all the system structures except the controller, such as the controlled plant, the actuator, and the weight function. In this paper, the control problem of the regeneratively-cooled scramjet engine is to track the command signal. Therefore, the block diagram of H_∞ standard problem considering instruction tracking is shown in Fig. 5, and the closed-loop control system can be described as

$$\begin{bmatrix} z \\ v \end{bmatrix} = P(s) \begin{bmatrix} w \\ u \end{bmatrix} = \begin{bmatrix} P_{11}(s) & P_{12}(s) \\ P_{21}(s) & P_{22}(s) \end{bmatrix} \begin{bmatrix} w \\ u \end{bmatrix} \quad (5)$$

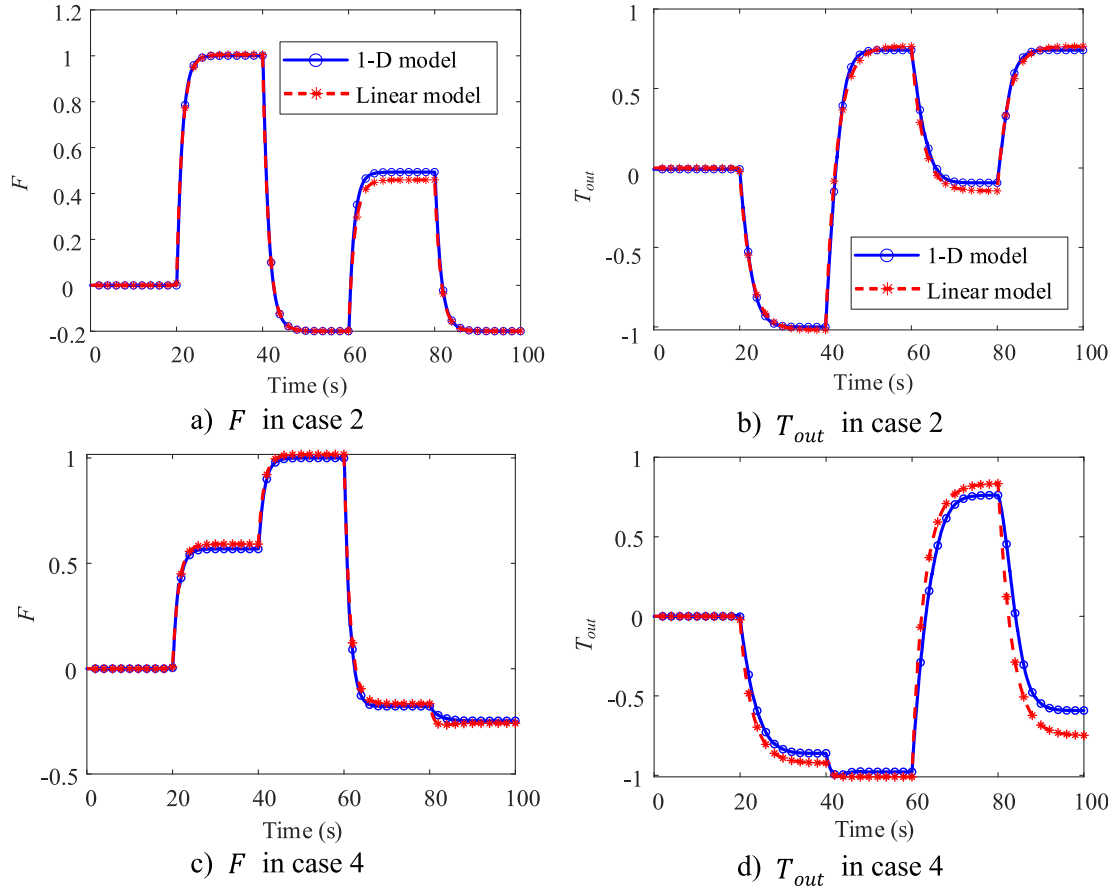


Fig. 4. The comparisons of thrust F and kerosene temperature at cooling channels outlet T_{out} between 1-D and linear model at Ma 6.

Table 3
The transfer functions of regeneratively-cooled scramjet engine for Case 1–4.

	Case 1	Case 3	Case 2	Case 4
$f_{11}(s)$	$\frac{0.2915}{s + 0.7568}$	$\frac{0.5374}{s + 0.7478}$	$g_{11}(s)$	$\frac{0.6302}{s + 0.7827}$
$f_{12}(s)$	$\frac{0.462}{s + 0.7473}$	$\frac{0.2135}{s + 0.7577}$	$g_{12}(s)$	$\frac{0.1135}{s + 0.568}$
$f_{21}(s)$	$\frac{-0.8561}{s + 0.8121}$	$\frac{-0.7989}{s + 0.8169}$	$g_{21}(s)$	$\frac{-0.09464}{s + 0.3732}$
$f_{22}(s)$	$\frac{0.03676}{s + 0.7033}$	$\frac{0.01665}{s + 0.7896}$	$g_{22}(s)$	$\frac{-0.2881}{s + 0.3761}$
				$\frac{0.6425}{s + 0.7555}$
				$\frac{0.1023}{s + 0.6151}$
				$\frac{-0.1871}{s + 1.086}$
				$\frac{-0.2694}{s + 0.3217}$

$$u = K(s)v \tag{6}$$

where $P(s)$ is the generalized controlled plant, $K(s)$ is the controller, w is the external input signal, u is the controller output signal, z is the performance output signal, and v is the controller input signal.

In Fig. 5, there are three weight functions, namely performance weight function W_1 , input weight function W_2 and output weight function W_3 . In general, H_∞ synthesis needs to examine the transfer function from the external input w to the performance output z . The transfer function from w to z can be expressed by a linear fractional transformation

$$z = F_l(P, K)w \tag{7}$$

where

$$F_l(P, K) = P_{11} + P_{12}K(I - P_{22}K)^{-1}P_{21} \tag{8}$$

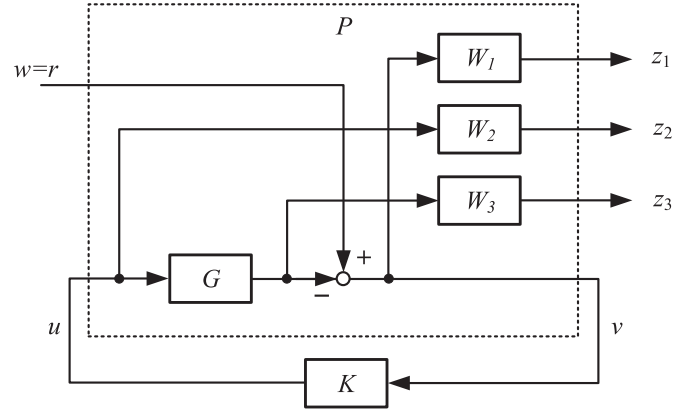


Fig. 5. The block diagram of H_∞ standard problem considering instruction tracking.

From Fig. 5, it is not difficult to know the element of generalized controlled plant $P(s)$ is

$$\begin{matrix} P_{11} = \begin{bmatrix} W_1 \\ 0 \\ 0 \end{bmatrix} & P_{12} = \begin{bmatrix} -W_1G \\ W_2 \\ W_3G \end{bmatrix} \\ P_{21} = I & P_{22} = -G \end{matrix} \tag{9}$$

By substituting equation (9) into equation (8), the transfer function from w to z can be obtained as follow

$$F_i(P, K) = \begin{bmatrix} W_1(I + GK)^{-1} \\ W_2K(I + GK)^{-1} \\ W_3GK(I + GK)^{-1} \end{bmatrix} \quad (10)$$

Among them, $S = (I + GK)^{-1}$ is the sensitivity function, and $T = GK(I + GK)^{-1}$ is the complementary sensitivity function that known as the closed-loop transfer function of the system. Obviously, $I = T + S$.

In robust control, the sensitivity function S can quantitatively characterize the sensitivity of the closed-loop transfer function T to the parameter changes of the controlled plant. Meanwhile, the sensitivity function S contains information such as the suppression characteristics of the closed-loop system against disturbances, and the tracking error for the input command signal. When S of the system is low, the designed controller has strong robustness to the modeling error of the controlled plant.

Further, equation (10) can be rewritten as

$$F_i(P, K) = \begin{bmatrix} W_1S \\ W_2KS \\ W_3T \end{bmatrix} \quad (11)$$

Referring to the general control structure shown in Fig. 5, the optimal control of the standard H_∞ problem is to find a stabilizing controller K that can minimize the following equation

$$F_i(P, K)_\infty = \max_\omega \bar{\sigma}(F_i(P, K)(j\omega)) \quad (12)$$

where \cdot_∞ is the H_∞ norm, which means the peak of the maximum singular value $\bar{\sigma}$ of $F_i(P, K)(j\omega)$. The stabilizing controller K can be solved by the theory called weighted H_∞ mixed sensitivity problem [38].

4.2. H_∞ control with structural uncertainty

$$F_i(P, K) = \begin{bmatrix} -W_1KG(I + KG)^{-1}W_1K(I + GK)^{-1} - W_1G(I + KG)^{-1} - W_1G(I + KG)^{-1} - W_2KG(I + KG)^{-1} & & \\ W_1(I + GK)^{-1} - W_2KG(I + KG)^{-1} - W_2KG(I + KG)^{-1} & & \\ & & W_3G(I + KG)^{-1} \end{bmatrix} \begin{bmatrix} W_2K(I + GK)^{-1} \\ W_3GK(I + GK)^{-1} \end{bmatrix} \quad (17)$$

There are always differences between the nominal model that used in the design of the controller to the actual system. This difference is also called model uncertainty. H_∞ robust control can consider the worst-case uncertainty and synthesize a control system that meets the design index. The method used is as follows:

- 1). The uncertainty set should be determined at first. Finding the mathematical expression of the model uncertainty is indispensable, which means clarifying what is known about less clear issues.
- 2). Combining the nominal model and uncertainty set to a neo-generalized controlled plant P . So that, the standard H_∞ control problem is reconstructed.
- 3). According to the design index, selecting the weight function to iteratively calculate the stabilizing controller K which can minimize equation (12) or satisfy the suboptimal control problem presented in this section.

First of all, for the uncertainty of the system, considering the structured multiplicative input uncertainty Δ_I . The system transfer function is can be converted to

$$G_p = G(1 + \Delta_I W_I) \quad (13)$$

where the W_I is the normalized uncertainty weight function. Meanwhile, the structured multiplicative input uncertainty can be expressed as $\Delta_I = \text{diag}(\Delta_i)$, and i is the dimension of the system input.

Generally, assuming that each perturbation is stable and normalized as follow

$$\bar{\sigma}(\Delta_i(j\omega)) \leq 1 \quad \forall \omega \quad (14)$$

Namely, the H_∞ norm of the structured multiplicative input uncertainty Δ_{I_∞} is not greater than one.

Secondly, the new control system and the H_∞ standard control problem block diagram are shown in Fig. 6 and Fig. 7, respectively. Where W_1 , W_2 , and W_3 are the normalized performance weight functions.

The neo-generalized controlled plant P consists of input variables $[u_\Delta, w, u]^T$ and output variables $[y_\Delta, z, v]^T$ in Fig. 7, where u_Δ is the uncertainty output signal and y_Δ is the uncertainty input signal. Simultaneously, Fig. 6 indicates the neo-generalized controlled plant P as follow

$$\begin{bmatrix} y_\Delta \\ z \\ v \end{bmatrix} = \begin{bmatrix} P_{11} & P_{12} \\ P_{21} & P_{22} \end{bmatrix} \begin{bmatrix} u_\Delta \\ w \\ u \end{bmatrix} \quad (15)$$

where

$$P_{11} = \begin{bmatrix} 0 & 0 \\ -W_1G & W_1 \\ 0 & 0 \\ W_3G & 0 \end{bmatrix} \quad (16)$$

$$P_{21} = [-G \quad I]$$

$$P_{22} = -G$$

By substituting equation (16) into equation (8), the transfer function from $[u_\Delta \quad w]^T$ to $[y_\Delta \quad z]^T$ can be obtained as follow

Thirdly, by assuming that γ_{min} is the minimum value relative to all stabilizing controllers for $F_i(P, K)_\infty$, the optimal control of H_∞ problem is transformed into the sub-optimal one: Finding all the stabilizing controllers that can satisfy the following equation

$$F_i(P, K)_\infty < \gamma \quad (18)$$

where $\gamma > \gamma_{min}$.

The algorithm proposed in Refs. [38,39], can solve H_∞ control problem efficiently. By iteratively reducing γ , an approximate optimal

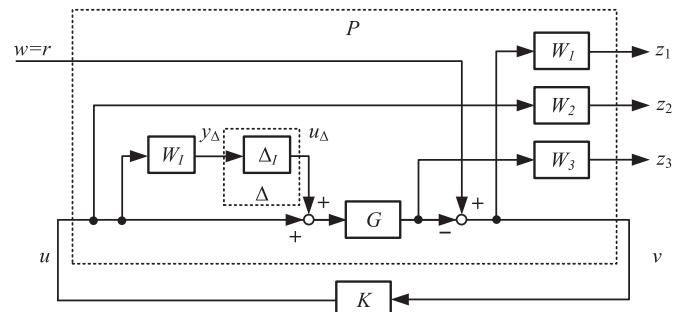


Fig. 6. The diagram of the H_∞ control system with structural uncertainty.

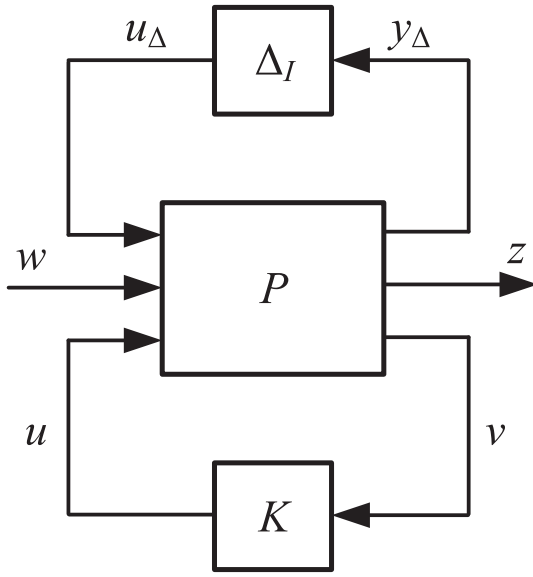


Fig. 7. The diagram of the standard H_∞ control problem with structural uncertainty.

solution can be obtained. The performance of the controller depends on the guarantee of the weight function. Therefore, based on the dynamic characteristics of the controlled plant, namely the regeneratively-cooled scramjet engine, a reasonable weight function should be selected to complete the design of the control system.

4.3. Multivariable switching controller based on output signal reset

The control strategy presented in this paper shows that it is difficult to solve the control problem of the regeneratively-cooled scramjet engine with a single multivariable controller. In order to deal with this issue, the switching controller should be considered to the engine during the entire flight climbing process. Thus, the stability of the switching control system is an important issue. The Lyapunov stability criterion given by modern control theory shows that the monotonicity decline of Lyapunov function on the trajectory of parameters is the guarantee of system stability. The switching system can guarantee the stability of the switching system through the common Lyapunov function [40] and the multiple Lyapunov function approach [41]. The multiple Lyapunov function method based on average dwell time can effectively reduce the conservativeness of the control system, which has been widely studied in ensuring the stability of switched systems and has been applied well in a series of LPV systems [34,35]. Interested researchers can further consult relevant literatures.

Suppose the following switched system

$$\dot{\eta} = A_\delta \eta \quad (19)$$

where $\eta \in \mathbb{R}^{n \times n}$ is state variable, δ is switching signal that takes the value in positive integer set $Z = \{1, \dots, N\}$. When $\delta = i$, it indicates that the i -th subsystem is activated and become to work.

Theorem 5.1 [41]: If there is a positive definite symmetric matrix $P_{cl} \in \mathbb{R}^{n \times n}$ satisfies

$$A_\delta^T P_{cl,\delta} + P_{cl,\delta} A_\delta + \frac{dP_{cl,\delta}}{dt} < 0 \quad (20)$$

switched system (19) is asymptotically stable during switching. If the Lyapunov function is independent of time, the above equation is equivalent to

$$A_\delta^T P_{cl,\delta} + P_{cl,\delta} A_\delta < 0 \quad (21)$$

By finding multiple positive definite symmetric matrices $P_{cl,\delta}$ that make the multiple Lyapunov functions are monotonically decreasing in their regions, the stability of the whole switched system can be kept. Obviously, the controllers designed in this paper have attenuated Lyapunov function, which ensures the stability of the switched control system. However, in the simulation process, the different sub-controllers are simultaneously calculating. If the output parameters of the sub-controllers differ too much, it is very likely to cause a nonlinear jump. Thus, further switching rules need to be considered to minimize or avoid this problem. In most cases, the time of system switching is determined by the working state of the controlled plant and is not directly related to the parameters of the sub-controller. Absolutely, it brings the freedom of sub-controller design. However, due to the independent design of each sub-controller, the continuity of the control output signal cannot be guaranteed infallibly when switching occurs. Therefore, a special controller output signal u reset link needs to be designed for ensuring the non-disturbance switching of the control system.

During the switching process, the output value of the previous controller will be used as the initial output value of the next controller, which is the main idea of controller switching method based on output signal reset. Fig. 8 indicates the scheme diagram of the switching control system based on output signal reset. Where, SF is the scale transformation module that referring to equation (2), SF^{-1} is the inverse scale transformation of SF, and the two control loops are distinguished by subscript "1" and "2". Meanwhile, y_r is the command signal, u is the controller output signal, e is the error signal, and δ is the switch command signal. Because the data used in the controller design are normalized results, the definition of symbols for the SF in Fig. 8 is equal to equation (2).

The output signal reset process is given below. In order to ensure the continuity of the controller output signal, u_2 should be equal to u_1 during the switching. As shown in Fig. 8, u_1 is converted to $\bar{u}_{2,1}$ through the SF_2 module, namely

$$\bar{u}_{2,1} = (u_1 - u_{2,0}) / \max(\text{abs}(u_2 - u_{2,0})) \quad (22)$$

Let \bar{u}_2 be equal to $\bar{u}_{2,1}$, then u_2 can be obtained through the SF_2^{-1} module as follows

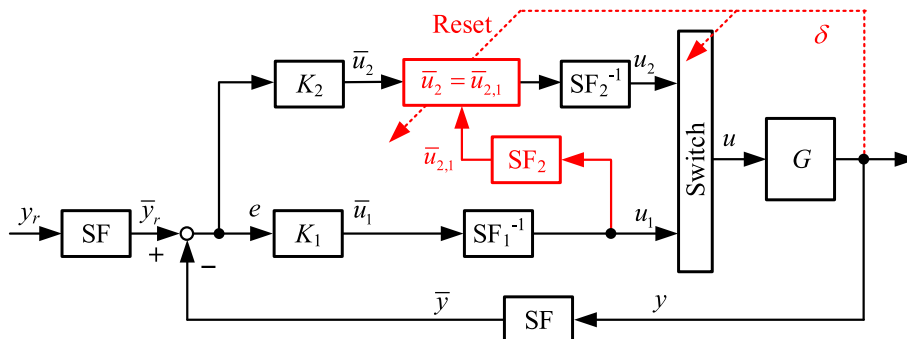


Fig. 8. Scheme diagram of the switching control system based on output signal reset.

$$u_2 = \bar{u}_{2,1} + u_{2,0} \quad (23)$$

So far, the u_2 obtained at switching time is the same as u_1 , which can guarantee that no sudden jump is in the controller output signal u . Besides, the identification results of the linear system also suggest that the variable range of the input signals of the two subsystems is identical. Therefore, as long as the performance index γ of the controller is not significantly various, there is no obvious difference in the magnitude of the controller output signal u before and after switching.

characteristics of the controlled plant and select the appropriate weight function for synthesis. The characteristics of the regeneratively-cooled scramjet engine are discussed, and the linear models are obtained in section 2.2. In this part, the weight functions are introduced in detail for H_∞ synthesis. However, if all the weight functions given in Fig. 6 is considered, the conservativeness of the control system is generally increased, which is not conducive to improving the control performance. In order to deal with this issue, W_1 and W_2 is selected as the weight functions. The transfer function in equation (17) can be simplified as follow

$$F_i(P, K) = \begin{bmatrix} -W_1KG(I+KG)^{-1}W_1K(I+GK)^{-1} - W_1G(I+KG)^{-1} - W_1G(I+KG)^{-1} - W_2KG(I+KG)^{-1} \\ W_1(I+GK)^{-1} - W_2KG(I+KG)^{-1} - W_2KG(I+KG)^{-1} \\ W_2K(I+GK)^{-1} \end{bmatrix} \quad (24)$$

5. Design and validation results

In this section, the switching H_∞ control with uncertain structure is applied to solve the control problem of the regeneratively-cooled scramjet engine under broad operating conditions. Firstly, according to the control strategy determined in section 2.1, the control loops under two different tasks are designed. There are the thrust and stability margin control loop, and the thrust and kerosene temperature control loop. Then, the switching multivariable control system of the engine is proposed, which can satisfy the operating condition from low Mach number to high. Finally, the control system is verified on the regeneratively-cooled scramjet engine 1-D model under both steady and unsteady conditions.

5.1. Thrust and steady margin control loop

When inlet steady margin ξ is close to the unstart boundary at low Mach number, it is significant to ensure the thrust F and inlet steady margin ξ . The scheme diagram of the thrust and steady margin control loop is shown in Fig. 9. According to the flight mission, the corresponding thrust command signal F_r and inlet steady margin command signal ξ_r can be selected. The difference between the command signal and the calculated result of the regeneratively-cooled scramjet engine 1-D model is the input of the controller. Subsequently, the controller completes the control of the closed-loop system by adjusting first and second stage fuel equivalence ratio, namely ϕ_1 and ϕ_2 . The linear model used for control system design is shown in equation (3).

There are two control objectives thrust F and steady margin ξ in this control loop. For F , it is the core target of the engine control, because the main task of a hypersonic vehicle is to provide the required thrust during the acceleration, cruise and son on. For fixed geometry engine, thrust can only be regulated by adjusting kerosene flow rate and injector position.

The key to the design of the H_∞ control system is to analyze the

The corresponding weight function is selected as follows

$$W_1 = \text{diag} \left\{ 2 \frac{s+0.4}{s+4}, 2 \frac{s+0.4}{s+4} \right\} \quad (25)$$

$$W_1 = \text{diag} \left\{ 0.5 \frac{s+1.2}{s+0.0003}, 0.5 \frac{s+1.2}{s+0.0003} \right\} \quad (26)$$

$$W_2 = \text{diag} \{ 0.5, 0.5 \} \quad (27)$$

The reason for the weight function selecting that discussed in Ref. [42] is given as follows:

Uncertainty weight function W_1 : The linearized model of the nonlinear system usually ignores unknown dynamic characteristics of higher or infinite orders. To represent these characteristics, a simple multiplicative function like equation (25) can be considered for each input and output channel. The unmodeled characteristic discussed in this section has a relative uncertainty of 20% at steady state and the frequency is about 2 rad/s when the relative uncertainty reaches 100%. At the same time, due to the omitted or inherently uncertain dynamic characteristics, the amplitude of the weight function is considered to be 2 at high frequencies.

Performance weight function W_1 : It is also known as the sensitivity weight function and can be approximated as the reciprocal of the desired sensitivity function. Generally speaking, in order to obtain the tracking accuracy of each controlled output, the control system requires a small sensitivity function. Meanwhile, the controller requires an integrator in the weight function related to the controlled output, so that the closed-loop system has the integral action. However, it is not necessary to ensure the steady-state error to be zero, so the weight functions produce a finite gain of 2000 in the low frequencies. Note that W_1 cannot contain pure integrals in any case, otherwise the standard H_∞ optimal control problem cannot be formed well when the corresponding generalized

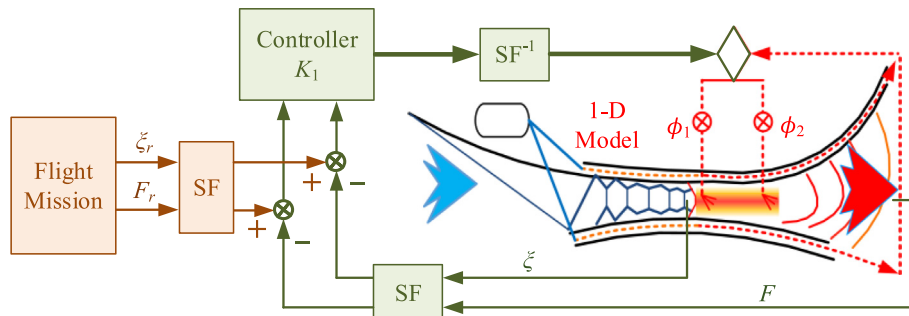


Fig. 9. Scheme diagram of the thrust and steady margin control loop.

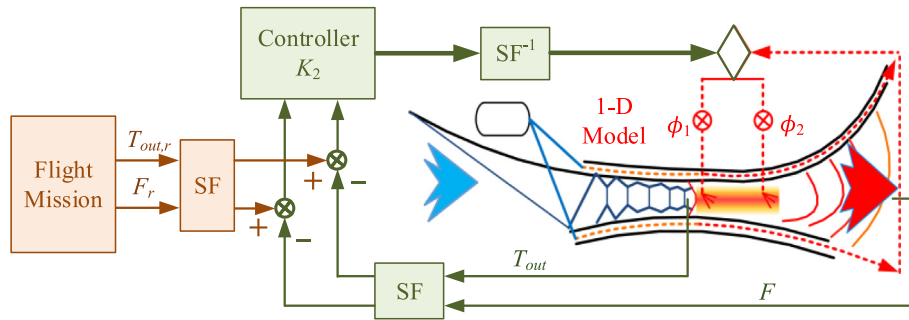


Fig. 10. Scheme diagram of the thrust and fuel temperature control loop.

controlled plant P cannot be stabilized by the feedback controller K . Therefore, the process of tuning W_1 shows that using a high-gain and low-pass filter on the main channel can improve the tracking accuracy to about 0.6 rad/s.

Performance weight function W_2 : It is also known as the input weight function. The main purpose of W_2 is to limit the amplitude of the input u . For the normalized system, the unit diagonal matrix is generally selected as the input weight function. Nevertheless, the linear model identified in this paper starts from zero, but not from zero to one. Thus, the weight function should be half of the identity matrix, which is $diag\{0.5, 0.5\}$.

According to the above weight functions, the corresponding controller K_1 is solved by H_∞ technology. The controller design index H_∞ norm γ is 2.062. This result not only satisfies the above-mentioned control system design index, but ensures the amplitude of the system uncertainty is 2 in the high frequencies.

5.2. Thrust and fuel temperature control loop

At high Mach number, the inlet steady margin ξ is moving away from the unstart boundary and the kerosene temperature at cooling channels outlet T_{out} is close to the overtemperature boundary. Thus, the issue turns into the control of engine thrust F and kerosene temperature at cooling channels outlet T_{out} . The scheme diagram of the thrust and fuel temperature control loop is shown in Fig. 10. The linear model used for control system design is demonstrated in equation (4).

There are two control objectives thrust F and kerosene temperature at cooling channels outlet T_{out} in this control loop. The particular content of this control loop is T_{out} . Kerosene temperature at cooling channels outlet is highest in 1-D model, so temperature monitoring point is located at the outlet of cooling channels. The purpose of temperature protection is to keep high performance of the engine without overtemperature phenomenon. In this way, kerosene can be in deep cracking state. It not only makes the best of heat sink of kerosene, but also has good atomization effect and high combustion efficiency after injected into combustor. The corresponding weight functions is equal to equation 25–27.

According to the above weight function, the corresponding controller K_2 is solved by H_∞ technology. The controller design index H_∞ norm γ is 2.063. This result also satisfies the above-mentioned control system design index, and ensures the amplitude of the system uncertainty is 2 in the high frequencies.

5.3. Design of switching multivariable controller

The regeneratively-cooled scramjet engine needs to consider different control loops under a wide range of operating conditions. Especially when the controlled output variables change, the switching between two sub-controllers is necessary. According to the multivariable switching controller based on output signal reset given in section 3.3, the scheme diagram of the switching control system is expressed in Fig. 11.

At low Mach numbers, the controller K_1 uses φ_1 and φ_2 to control the engine thrust F and inlet steady margin ξ . At high Mach numbers, the controller K_2 uses φ_1 and φ_2 to control the engine thrust F and kerosene temperature at cooling channels outlet T_{out} . Generally, the inlet steady margin ξ is expected to operate close to the unstart boundary for maximize engine performance. With the increase of the flight Mach number, the shock wave in the inlet is gradually pushed away, the steady margin ξ increases, and the engine keeps away from the unstart boundary. The inlet steady margin ξ is no longer the main target of the control system, which means the control system need to switch from K_1 to K_2 . In addition, the switching system needs to determine the switching signal. The control strategy of the engine is to ensure safe operation with high performance. As a result, the engine needs to work close to the safe boundary, that is, a small inlet steady margin ξ . During this operating condition, the kerosene temperature at cooling channels outlet T_{out} changes significantly with ξ . Choosing the ξ as switching signal is not conducive to solving the overtemperature. Therefore, T_{out} is set as the switching signal in switching controller. In this paper, when kerosene temperature at cooling channels outlet T_{out} is greater than 815 K, the switching is triggered.

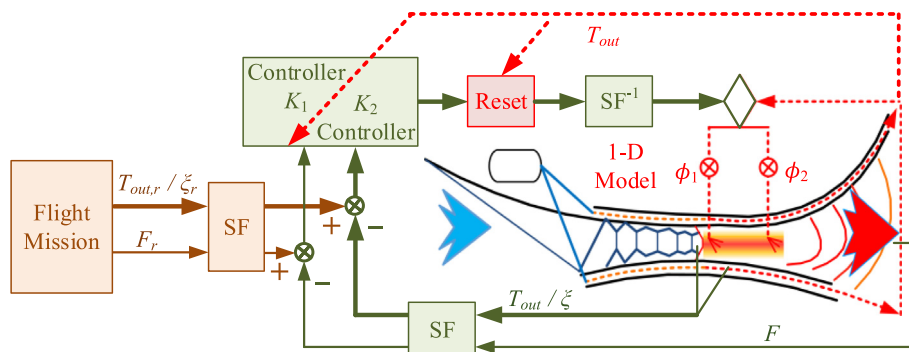


Fig. 11. Scheme diagram of the switching control system.

5.4. Validation of control system

The validation of the control system is carried out on the regeneratively-cooled scramjet engine 1-D model. It is assumed that $\varphi_{total} = \varphi_1 + \varphi_2$ is no more than 1.1 in simulations. This limit refers to Ref. [9]. The flight conditions of the 1-D model are shown in Table 1. The validations of the control system at specific operating conditions and variable operating conditions are given as follow.

A). Specific operating conditions

The thrust and steady margin control loop is verified at Ma 4.5. Dynamic responses of thrust F , inlet steady margin ξ , first stage fuel equivalence ratio and φ_1 , and second stage fuel equivalence ratio φ_2 are shown in Fig. 12-Fig. 14.

Fortunately, the thrust and steady margin control loop have achieved satisfactory control results. Fig. 12 shows that the control system can ensure the steady-state error of the engine thrust F close to zero. The duration of the thrust tracking to the steady-state value is about 4 s,

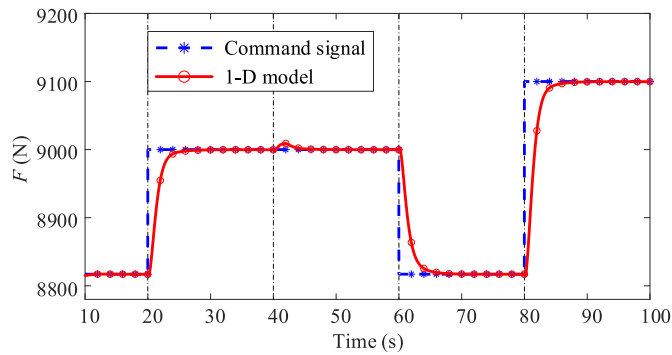


Fig. 12. Dynamic response of thrust F in multivariable control system (K_1).

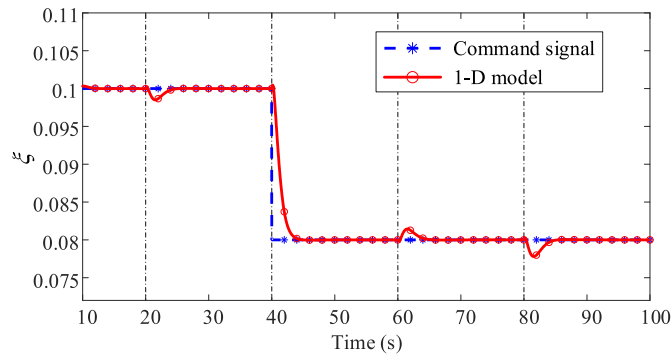


Fig. 13. Dynamic response of inlet steady margin ξ in multivariable control system (K_1).

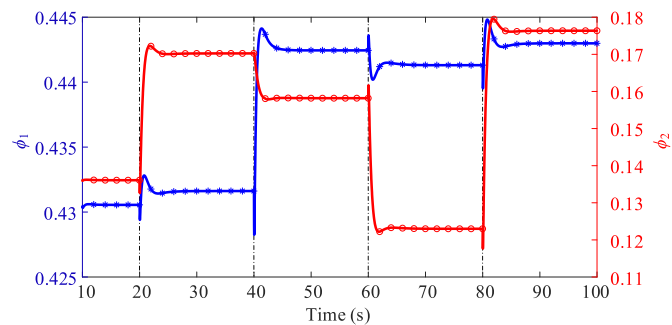


Fig. 14. Dynamic response of first and second stage fuel equivalence ratio (φ_1 and φ_2) in multivariable control system (K_1).

which is close to the dynamic characteristics of the engine. It can be seen that the control system responds quickly and meets the needs of rapid maneuvering. When another command signal ξ_r changes, the amount of thrust overshoot is less than 10 N at 40 s, and the thrust returns to the control command value at about 3 s. In addition, the response of the ξ expressed in Fig. 13 has similar indicators. The steady-state error of the ξ is close to zero. The duration of the ξ tracking to the steady-state value is about 4 s. When the thrust command signal F_r is changing, the ξ has no significant overshoot. Meanwhile, the sum of the two-stage fuel equivalence ratios does not exceed the limit value 1.1 in Fig. 14.

The thrust and fuel temperature control loop is verified at Ma 6. Dynamic responses of thrust F , kerosene temperature at cooling channels outlet T_{out} , first stage fuel equivalence ratio and φ_1 and second stage fuel equivalence ratio φ_2 are shown in Fig. 15-17

Although the control effect of the thrust and fuel temperature control loop is not as good as the thrust and steady margin control loop, it also basically meets the control requirements of the system. The steady-state error of the engine thrust F is close to zero in Fig. 15. Due to the influence of rising kerosene temperature and kerosene cracking, the settling time of

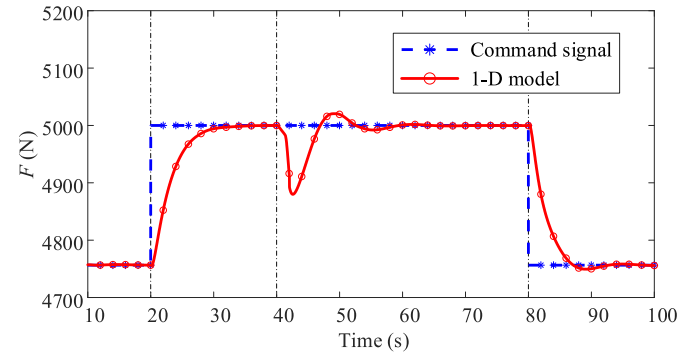


Fig. 15. Dynamic response of thrust F in multivariable control system (K_2).

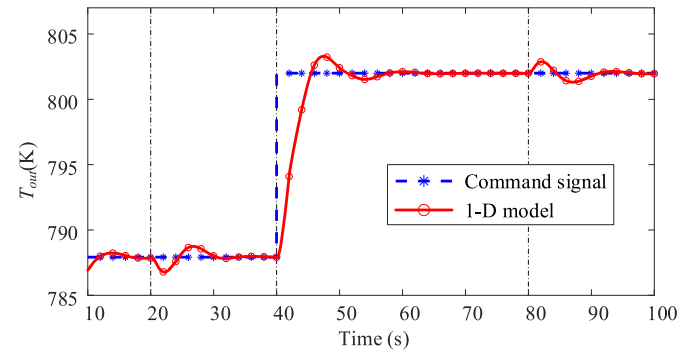


Fig. 16. Dynamic response of kerosene temperature at cooling channels outlet T_{out} in multivariable control system (K_2).

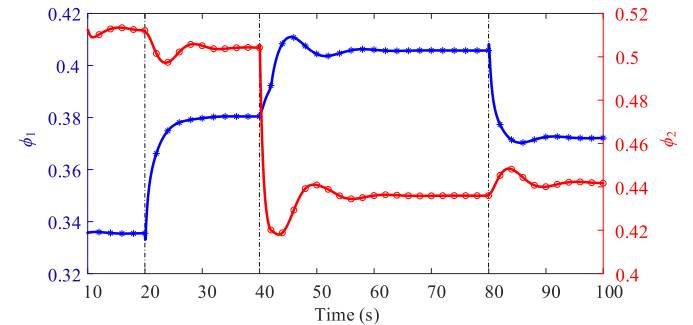


Fig. 17. Dynamic response of first and second stage fuel equivalence ratio (φ_1 and φ_2) in multivariable control system (K_2).

the engine increases, which is also reflected in the identification results of the linear model in Figs. 3 and 4. The duration of the thrust tracking to the steady-state value is about 10 s, which is close to the dynamic characteristics of the engine. When another command signal $T_{out,r}$ changes, the amount of thrust overshoot is near 150 N at 40 s, and the thrust returns to the control command value at about 10 s. In order to make the setting time of the control system close to engine dynamics, an overshoot of about 10% occurs in the kerosene temperature at cooling channels outlet T_{out} in Fig. 15. The steady-state error of the T_{out} close to zero. The duration of the T_{out} tracking to the steady-state value is approximately 10 s. Similarly, the sum of the two-stage fuel equivalent ratios does not exceed the limit value 1.1 in Fig. 17.

The particularity of kerosene temperature at cooling channels outlet under high Mach number is a special control problem of regeneratively-cooled scramjet engines. It is also urgent to be solved. The high temperature of kerosene brings large inertia to the engine, and it is not recommended to change the command signal of kerosene temperature at cooling channels outlet T_{out} when temperature is close to the threshold value. Therefore, this paper adopts the equal fuel temperature command signal for the thrust and fuel temperature control loop in the process of engine acceleration.

In addition, the trajectory tracking problem of systems with unknown parameters and external disturbance involves many important issues about controller designs [43]. In particular, the disturbance/noise effect on the system. Therefore, noise interference is applied to the simulation process under the above conditions to verify the robustness of the control system. Figs. 18–20 show the thrust and steady margin control loop verification results under noise interference. Figs. 21–23 show the thrust and fuel temperature control loop verification results under noise interference. The results indicate that the system can ensure stability under the interference of random noise. The steady state error of each output is close to 0, the dynamic adjustment time has no obvious change, and the fluctuation of two-stage fuel equivalent ratio affected by noise is about

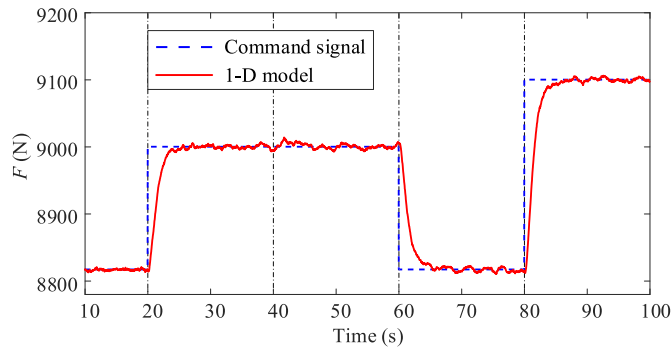


Fig. 18. Dynamic response of thrust F in multivariable control system with noise (K_1).

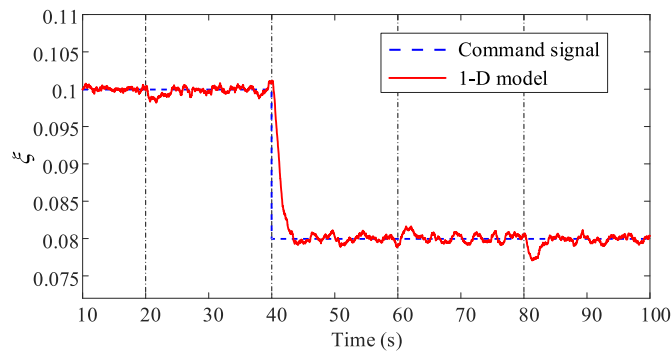


Fig. 19. Dynamic response of inlet steady margin ξ in multivariable control system with noise (K_1).

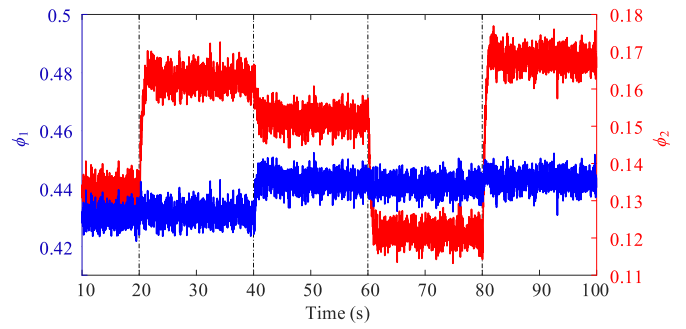


Fig. 20. Dynamic response of first and second stage fuel equivalence ratio (φ_1 and φ_2) in multivariable control system with noise (K_1).

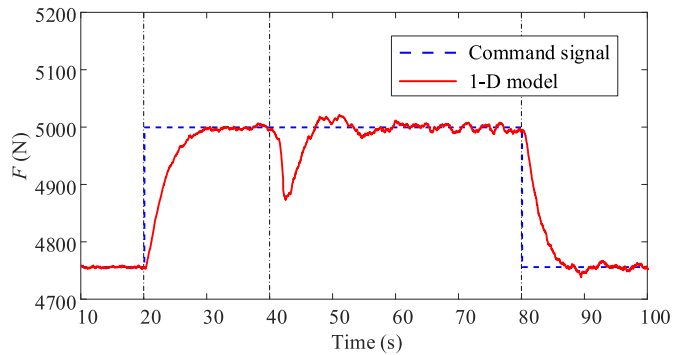


Fig. 21. Dynamic response of thrust F in multivariable control system with noise (K_2).

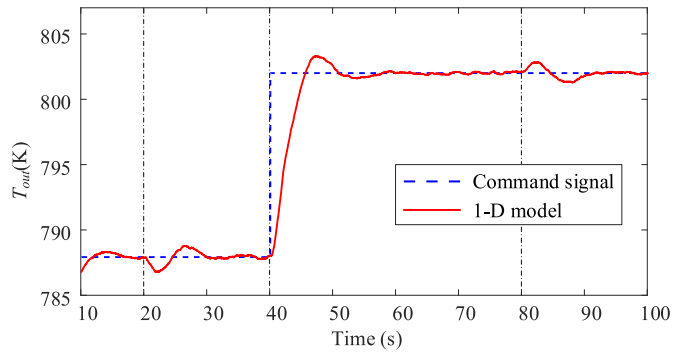


Fig. 22. Dynamic response of kerosene temperature at cooling channels outlet T_{out} in multivariable control system with noise (K_2).

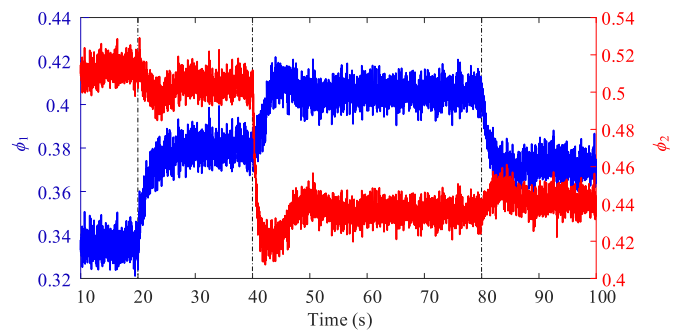


Fig. 23. Dynamic response of first and second stage fuel equivalence ratio (φ_1 and φ_2) in multivariable control system with noise (K_2).

1%. The robustness of controllers meets the requirements.

B). Variable operating conditions

With hypersonic vehicles operating in a wide range of operating conditions, it is not sufficient to verify only two control loops under specific operating conditions. Thus, the control system of the regeneratively-cooled scramjet engine is validated during the acceleration from Mach 4 to Mach 7. Fig. 24 indicates Mach number in validation. Dynamic responses of thrust F , inlet steady margin ξ , kerosene temperature at cooling channels outlet T_{out} , first stage fuel equivalence ratio and ϕ_1 , and second stage fuel equivalence ratio ϕ_2 are shown in Figs. 25-28.

The acceleration process of the system begins at 30 s from Mach 4. The thrust and steady margin command are shown in Figs. 25 and 26,

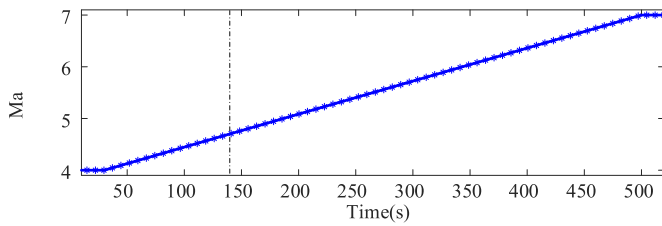


Fig. 24. Mach number in multivariable switching control system.

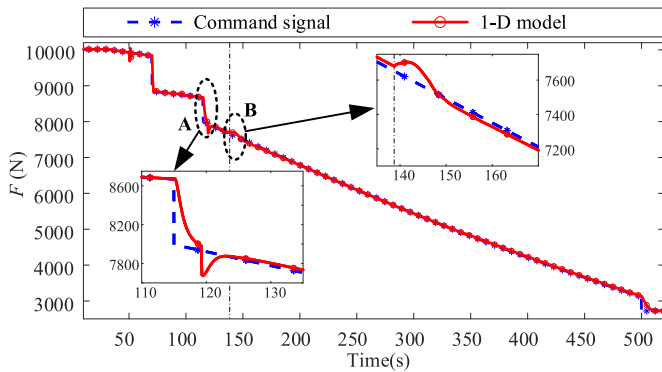


Fig. 25. Dynamic response of thrust F in multivariable switching control system.

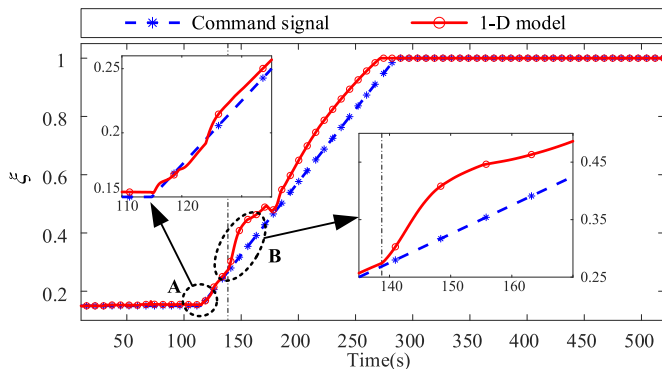


Fig. 26. Dynamic response of inlet steady margin ξ in multivariable switching control system.

separately. At 70 s, the thrust command F_r decreases from 9839 N to 8852 N. The response of engine thrust F adjusts quickly, and the inlet steady margin ξ is stabilized at about 0.15. As shown in region A, the thrust command F_r decreased from 8656 N to 7994 N again to verify the

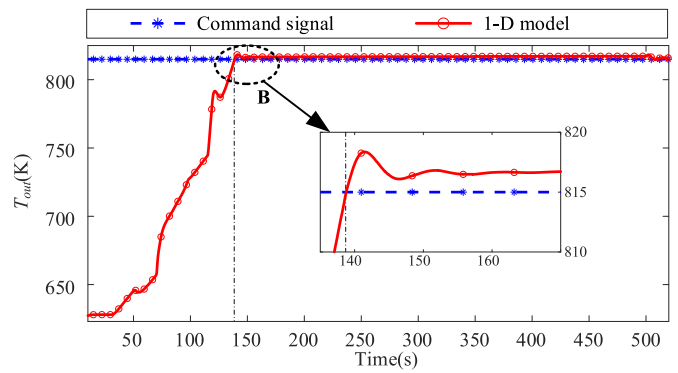


Fig. 27. Dynamic response of kerosene temperature at cooling channels outlet T_{out} in multivariable switching control system.

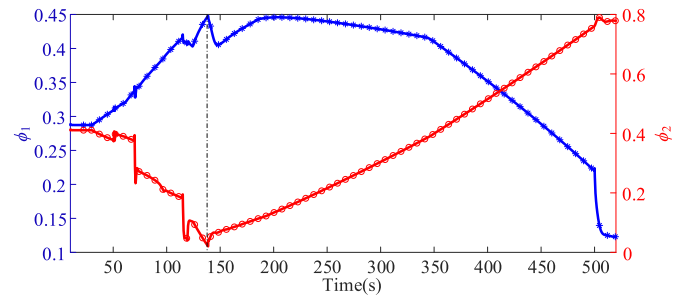


Fig. 28. Dynamic response of first and second stage fuel equivalence ratio (ϕ_1 and ϕ_2) in multivariable switching control system.

tracking performance of the control system at 115 s. It is worth noting that the engine thrust F has a step decrease of nearly 350 N at 120 s, which is because of the correction method used to handle the nonlinear positive shock wave in the 1-D model. The small thrust fluctuation at 50 s is also caused by this reason. However, the control system still has good effect, and the engine output F approaches the command signal F_r after 10 s. At this point, Fig. 26 indicates that the flight Mach exceeds 4.5, and the command signal ξ_r increases linearly. The inlet steady margin ξ calculated by the 1-D model can track ξ_r well. When the aircraft accelerates from Mach 4 to about 4.5, the kerosene temperature rapidly rises to about 750 K in Fig. 27, approaching the switching command threshold of 815 K. With the further acceleration of the aircraft in region B, the kerosene temperature at cooling channels outlet reaches the limit value at 139 s, and the closed-loop system is switched from controller K_1 to K_2 . The thrust command F_r keeps falling, while the command $T_{out,r}$ is kept at 815 K to avoid the danger of overtemperature. The results show that the switching process is stable and continuous. After switching, there is an overshoot of about 3 K in T_{out} . During the acceleration process, the error of T_{out} is maintained at about 1.5 K, which is satisfactory. In addition, the ξ does not change along the preset command after switching, but it is far away from the inlet unstart boundary during the operation. The acceleration ends at 500 s. Finally, Fig. 28 shows that the sum of the two-stage fuel equivalent ratios does not exceed the limit value 1.1.

As a whole, multivariable switching control system designed in this paper can control thrust, steady margin and kerosene temperature tracking the setting command signals. Engines can operate close to safety boundary and make good full use of potential performance. Reasonability and validity of multivariable switching control system are validated based on 1-D model for regeneratively-cooled scramjet engine. The whole engine system shows excellent control effect such as high response speed, smoothness, stability and so on. Meanwhile, the effectiveness of closed-loop system is verified not only in specific operating conditions, but also in acceleration from Mach 4 to Mach 7.

6. Conclusions

Regeneratively-cooled scramjet engine has some differences from non-cooled one. It is mainly the physical and chemical reactions involved in cooling kerosene, which brings about the overtemperature problem of control. Meanwhile, traditional issue of inlet unstart also plagues the controller designers of regeneratively-cooled scramjet engines at low Mach number. Hence, through the design of two control loops and the switching method based on controller output reset, a multivariable switching controller is established for the engine with two-stage kerosene injection. The effectiveness of the switching control system is verified both in specific and acceleration conditions. The main conclusions of this paper are summarized as follows:

- 1). This research divides the control problem of the regeneratively-cooled scramjet engine into two control loops at different Mach numbers. The multivariable controllers are designed in the thrust and steady margin control loop, as well as the thrust and fuel temperature control loop. By adjusting two stage kerosene allocation proportion reasonably, the inlet unstart issue and overtemperature issue of the regeneratively-cooled scramjet engine with high performance are solved, which is verified in specific operating conditions.
- 2). A multivariable switching controller for the regeneratively-cooled scramjet engine during acceleration is obtained. The switching controller based on output signal reset is proposed to work out the contradiction between high performance and safe operation under different operating conditions. The effectiveness of the control system is verified under variable operating conditions from Mach 4 to Mach 7. Meanwhile, the results show that the tracking accuracy of the controlled output thrust, inlet steady margin, and kerosene temperature at cooling channels outlet are satisfactory. In addition, the switching process is stable and smooth.

Credit author statement

Chengkun Lv: Methodology, Software, Investigation, Writing - original draft, Visualization. Juntao Chang: Conceptualization, Methodology, Software, Formal analysis, Visualization. Daren Yu: Conceptualization, Supervision, Formal analysis, Visualization. Hao Liu: Validation, Resources, Writing - review & editing, Supervision. Xu Cheng: Resources, Writing - review & editing, Supervision, Data curation.

Declaration of competing interest

The authors declare that they have no known competing financial interests or personal relationships that could have appeared to influence the work reported in this paper.

Acknowledgements

This research work is supported by the National Science and Technology Major Project (2017-V-0004-0054).

References

- [1] J.T. Chang, J.L. Zhang, W. Bao, D.R. Yu, Research progress on strut-equipped supersonic combustors for scramjet application, *Prog. Aero. Sci.* 103 (2018) 1–30.
- [2] W. Huang, L. Yan, J.G. Tan, Survey on the mode transition technique in combined cycle propulsion systems, *Aero. Sci. Technol.* 39 (2014) 685–691.
- [3] M.N. Khan, I. Tlili, New approach for enhancing the performance of gas turbine cycle: a comparative study, *Results in Engineering* (2019) 2.
- [4] J.R. Serrano, P. Piqueras, E.J. Sanchis, B. Diesel, A modelling tool for engine and exhaust aftertreatment performance analysis in altitude operation, *Results in Engineering* (2019) 4.
- [5] L. Taddeo, N. Gascoin, K. Chetehouna, A. Ingenito, F. Stella, M. Bouchez, B.L. Naour, Experimental study of pyrolysis-combustion coupling in a regeneratively cooled combustor: system dynamics analysis, *Aero. Sci. Technol.* 67 (2017) 473–483.
- [6] J.C. Ma, J.T. Chang, J.L. Zhang, W. Bao, D.R. Yu, Control-oriented unsteady one-dimensional model for a hydrocarbon regeneratively-cooled scramjet engine, *Aero. Sci. Technol.* 85 (2019) 158–170.
- [7] J.T. Chang, N. Li, K.J. Xu, W. Bao, D.R. Yu, Recent research progress on unstart mechanism, detection and control of hypersonic inlet, *Prog. Aero. Sci.* 89 (2017) 1–22.
- [8] W. Huang, Z. Chen, L. Yan, B.B. Yan, Z.B. Du, Drag and heat flux reduction mechanism induced by the spike and its combinations in supersonic flows: a review, *Prog. Aero. Sci.* 105 (2019) 31–39.
- [9] J.C. Ma, J.T. Chang, Q.P. Huang, W. Bao, D.R. Yu, Multi-objective coordinated control of regeneratively-cooled scramjet engine with two-stage kerosene injection, *Aero. Sci. Technol.* 90 (2019) 59–69.
- [10] D.J. Dalle, M.L. Fotia, J.F. Driscoll, Reduced-order modeling of two-dimensional supersonic flows with applications to scramjet inlets, *J. Propul. Power* 26 (3) (2010) 545–555.
- [11] F. Xing, C. Ruan, Y. Huang, X.Y. Fang, Y.F. Yao, Numerical investigation on shock train control and applications in a scramjet engine, *Aero. Sci. Technol.* 60 (2017) 162–171.
- [12] K.J. Xu, J.T. Chang, N. Li, W.X. Zhou, D.R. Yu, Experimental investigation of mechanism and limits for shock train rapid forward movement, *Exp. Therm. Fluid Sci.* 98 (2018) 336–345.
- [13] W. Huang, Z.G. Wang, M. Pourkashanian, L. Ma, D.B. Ingham, S.B. Luo, J. Lei, J. Liu, Numerical investigation on the shock wave transition in a three-dimensional scramjet isolator, *Acta Astronaut.* 68 (11–12) (2011) 1669–1675.
- [14] N. Li, J.T. Chang, K.J. Xu, D.R. Yu, W. Bao, Y.P. Song, Oscillation of the shock train in an isolator with incident shocks, *Phys. Fluids* 30 (11) (2018) 116102.
- [15] Z.G. Wang, M.B. Sun, H.B. Wang, J.F. Yu, J.H. Liang, F.C. Zhuang, Mixing-related low frequency oscillation of combustion in an ethylene-fueled supersonic combustor, *Proc. Combust. Inst.* 35 (2) (2015) 2137–2144.
- [16] Y. Tian, B.G. Xiao, S.P. Zhang, J.W. Xing, Experimental and computational study on combustion performance of a kerosene fueled dual-mode scramjet engine, *Aero. Sci. Technol.* 46 (2015) 451–458.
- [17] W. Huang, L. Yan, Numerical investigation on the ram-scram transition mechanism in a strut-based dual-mode scramjet combustor, *Int. J. Hydrogen Energy* 41 (8) (2016) 4799–4807.
- [18] B.G. Xiao, J.W. Xing, Y. Tian, X.Y. Wang, Experimental and numerical investigations of combustion mode transition in a direct-connect scramjet combustor, *Aero. Sci. Technol.* 46 (2015) 331–338.
- [19] Y. Tian, S.H. Yang, J.L. Le, T. Su, M.X. Yue, F.Y. Zhong, X.Q. Tian, Investigation of combustion and flame stabilization modes in a hydrogen fueled scramjet combustor, *Int. J. Hydrogen Energy* 41 (2016) 19218–19230.
- [20] S.M. Torrez, D.J. Dalle, J.F. Driscoll, New method for computing performance of choked reacting flows and ram-to-scram transition, *J. Propul. Power* 29 (2) (2015) 433–445.
- [21] J.C. Ma, J.T. Chang, J.L. Zhang, W. Bao, D.R. Yu, Control-oriented modeling and real-time simulation method for a dual-mode scramjet combustor, *Acta Astronaut.* 153 (2018) 82–94.
- [22] M. Varshney, M.F. Baig, Unstart control in scramjet engines, in: *AIAA SciTech Forum*, San Diego, California, 2019, p. 297.
- [23] H.K. Liu, C. Yan, Y.T. Zhao, S. Wang, Active control method for restart performances of hypersonic inlets based on energy addition, *Aero. Sci. Technol.* 85 (2019) 481–494.
- [24] L. Vanstone, K.E. Hashemi, J. Lingren, M.R. Akella, N.T. Clemens, J. Donbar, S. Gogineni, Closed-loop control of shock-train location in a combustor scramjet, *J. Propul. Power* 34 (3) (2017) 660–667.
- [25] N. Li, J.T. Chang, K.J. Xu, D.R. Yu, Y.P. Song, Closed-loop control of shock train in inlet-isolator with incident shocks, *Exp. Therm. Fluid Sci.* 103 (2019) 355–363.
- [26] Y.W. Qi, W. Bao, Q.X. Zhang, R.F. Cao, Command switching based multiobjective safety protection control for inlet buzz of scramjet engine, *J. Franklin Inst.* 352 (11) (2015) 5191–5213.
- [27] R.F. Cao, J.T. Chang, J.F. Tang, W. Bao, D.R. Yu, Z.Q. Wang, Switching control of thrust regulation and inlet unstart protection for scramjet engine based on Min strategy, *Aero. Sci. Technol.* 40 (2015) 96–103.
- [28] R.F. Cao, J.T. Chang, J.F. Tang, W. Bao, D.R. Yu, Z.Q. Wang, Switching control of thrust regulation and inlet unstart protection for scramjet engine based on strategy of integral initial values resetting, *Aero. Sci. Technol.* 45 (2015) 484–489.
- [29] J.A. Echols, K. Puttannaiah, K. Mondal, A.A. Rodriguez, Fundamental control system design issues for scramjet-powered hypersonic vehicles, in: *AIAA Guidance, Navigation, and Control Conference*, Kissimmee, Florida, 2015, p. 1760.
- [30] H. An, Q.Q. Wu, C.H. Wang, Differentiator based full-envelope adaptive control of air-breathing hypersonic vehicles, *Aero. Sci. Technol.* 82 (2018) 312–322.
- [31] A. Goel, K. Duraisamy, D.S. Bernstein, Retrospective cost adaptive control of unstart in a model scramjet combustor, *AIAA J.* 56 (3) (2018) 1085–1096.
- [32] S. Du, H.R. Karimi, J. Qiao, D. Wu, C. Feng, Stability analysis for a class of discrete-time switched systems with partial unstable subsystems, *IEEE Transactions on Circuits and Systems II: Express Briefs.* 66 (12) (2019) 2017–2021.
- [33] J. Zhang, X. Zhao, F. Zhu, H.R. Karimi, Reduced-Order observer design for switched descriptor systems with unknown inputs, *IEEE Trans. Automat. Contr.* 65 (1) (2020) 287–294.
- [34] D. Yang, G. Zong, H.R. Karimi, H-infinity refined antidisturbance control of switched LPV systems with application to aero-engine, *IEEE Trans. Ind. Electron.* 67 (4) (2020) 3180–3190.
- [35] Q. Lu, L. Zhang, P. Shi, H.R. Karimi, Control design for a hypersonic aircraft using a switched linear parameter-varying system approach, *Proc. Inst. Mech. Eng. Part I-J Syst Control Eng.* 227 (1) (2013) 85–95.

- [36] Z.G. Jin, K.Y. Zhang, Y. Liu, Design and performance investigation of sidewall compression scramjet inlets operating from Mach 4 to Mach 7, *J. Aero. Power* 26 (6) (2011) 1201–1208.
- [37] L. Zhang, K.Y. Zhang, L. Wang, Y. Wang, Numerical investigation of hypersonic curved shock sidewall compression inlet, *J. Aero. Power* 30 (2) (2015) 281–288.
- [38] J.C. Doyle, K. Glover, P.P. Khargonekar, State-space solutions to standard H₂ and H_∞ control problems, *IEEE Trans. Automat. Contr.* 8 (8) (1989) 831–847.
- [39] P. Gahinet, P. Apkarian, A linear matrix inequality approach to H_∞ control, *Int. J. Robust Nonlinear Control* 4 (4) (1994) 421–448.
- [40] P. Apkarian, P. Gahinet, G. Becker, Self-scheduled H_∞ control of linear parameter-varying systems: a design example, *Automatica* 31 (9) (1995) 1251–1261.
- [41] C.W. Scherer, LMI relaxation in robust control, *Eur.j.control* 1 (2006) 3–29.
- [42] S. Skogestad, I. Postlethwaite, *Multivariable Feedback Control: Analysis and Design*, John Wiley & Sons, Inc., 1996.
- [43] Z.J. Wu, H.R. Karimi, P. Shi, Practical trajectory tracking of random Lagrange systems, *Automatica* 105 (2019) 314–322.